Experimental validation of laminated composites with thermal and/or mechanical coupling response: a search for hygro-thermally curvature-stable designs.

Jérôme Rousseau
Institut Supérieur de l'Automobile et des Transports, Université de Bourgogne, Nevers, France

Georges Verchery
Institut Supérieur des Matériaux et Mécaniques Avancés, 44, Avenue Frédéric Auguste Bartholdi, 72000 Le Mans, France

Christopher B. York
Aerospace Sciences, University of Glasgow,
James Watt (South) Building
Glasgow G12 8QQ
Christopher.York@Glasgow.ac.uk

Summary

The main focus of this work is the identification and experimental validation of laminate configurations which possess complex mechanical couplings but remain hygro-thermally curvature-stable (HTCS) or warp-free.

HTCS laminates allow a broad range of exotic mechanical coupling attributes to be exploited without the complicating issue of thermal distortions, which are an inevitable consequence of the high temperature curing process.

Aero-elastic compliant rotor blades with tailored extension-twist coupling* is an example of one such laminate design that requires either specially curved tooling or hygro-thermally curvature-stable properties in order to remain flat (or possess the desired shape) after high temperature curing.

* Winckler, S. J. (1985) "Hygrothermally curvature stable laminates with tension-torsion coupling. *J. American Helicopter Society*, **31**: 56-58.

Characterisation of coupled laminates

Coupling behaviour is dependent on the form of the elements in each of the extensional (**A**), coupling (**B**) and bending (**D**) stiffness matrices:

$$\begin{Bmatrix} N_x \\ N_y \\ N_{xy} \end{Bmatrix} = \begin{bmatrix} \mathrm{A}_{11} & \mathrm{A}_{12} & \mathrm{A}_{16} \\ & \mathrm{A}_{22} & \mathrm{A}_{26} \\ \text{Sym.} & & \mathrm{A}_{66} \end{bmatrix} \begin{Bmatrix} \varepsilon_x \\ \varepsilon_y \\ \gamma_{xy} \end{Bmatrix} + \begin{bmatrix} \mathrm{B}_{11} & \mathrm{B}_{12} & \mathrm{B}_{16} \\ & \mathrm{B}_{22} & \mathrm{B}_{26} \\ \text{Sym.} & & \mathrm{B}_{66} \end{bmatrix} \begin{Bmatrix} \kappa_x \\ \kappa_y \\ \kappa_{xy} \end{Bmatrix}$$

$$\begin{Bmatrix} M_x \\ M_y \\ M_{xy} \end{Bmatrix} = \begin{bmatrix} \mathrm{B}_{11} & \mathrm{B}_{12} & \mathrm{B}_{16} \\ & \mathrm{B}_{22} & \mathrm{B}_{26} \\ \text{Sym.} & & \mathrm{B}_{66} \end{bmatrix} \begin{Bmatrix} \varepsilon_x \\ \varepsilon_y \\ \gamma_{xy} \end{Bmatrix} + \begin{bmatrix} \mathrm{D}_{11} & \mathrm{D}_{12} & \mathrm{D}_{16} \\ & \mathrm{D}_{22} & \mathrm{D}_{26} \\ \text{Sym.} & & \mathrm{D}_{66} \end{bmatrix} \begin{Bmatrix} \kappa_x \\ \kappa_y \\ \kappa_{xy} \end{Bmatrix}$$

and may be described by a response based labelling system or compact matrix notation[†].

[†] ESDU (1994). Stiffnesses of laminated plates, Engineering Sciences Data Unit, Item No. 94003.

Unique coupling responses, due to free thermal contraction.

$\mathbf{A}_S\mathbf{B}_0\mathbf{D}_S$	$\mathbf{A}_S\mathbf{B}_l\mathbf{D}_S$	$\mathbf{A}_S\mathbf{B}_t\mathbf{D}_S$	$\mathbf{A}_S\mathbf{B}_{lt}\mathbf{D}_S$	$\mathbf{A}_S\mathbf{B}_S\mathbf{D}_S$	$\mathbf{A}_S\mathbf{B}_F\mathbf{D}_S$
$[+_2/-/\bigcirc/-_2/+]_T$	$[+/-/\bigcirc/-/\bigcirc/+/\bullet/+/-]_T$	$[+/-]_T$	$[+/\bigcirc/\bullet/-]_T$	$[+/-_2/\bigcirc/+_2/-/\bullet]_T$	$[+/-_2/+/\bigcirc/+/-/\bullet]_T$

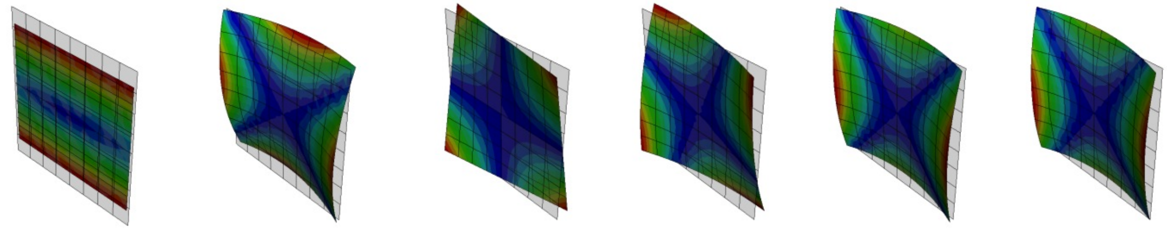

Simple laminate	*B-E*	*B-S-T-E*	*B-E-B-S-T-E*	*B-E-T-S*	*B-E-B-S-T-E-T-S*
$\mathbf{B} = \mathbf{0}$	$\begin{bmatrix} B_{11} & 0 & 0 \\ 0 & B_{22} & 0 \\ 0 & 0 & 0 \end{bmatrix}$	$\begin{bmatrix} 0 & 0 & B_{16} \\ 0 & 0 & B_{26} \\ B_{61} & B_{62} & 0 \end{bmatrix}$	$\begin{bmatrix} B_{11} & 0 & B_{16} \\ 0 & B_{22} & B_{26} \\ B_{61} & B_{62} & 0 \end{bmatrix}$	$\begin{bmatrix} B_{11} & B_{12} & 0 \\ B_{21} & B_{22} & 0 \\ 0 & 0 & B_{66} \end{bmatrix}$	$\begin{bmatrix} B_{11} & B_{12} & B_{16} \\ B_{21} & B_{22} & B_{26} \\ B_{61} & B_{62} & B_{66} \end{bmatrix}$

Coupling responses, due to free thermal contraction, for laminates with bending-twisting coupling (or *B-T* laminate) combined with:

$\mathbf{A}_S\mathbf{B}_0\mathbf{D}_F$	$\mathbf{A}_S\mathbf{B}_l\mathbf{D}_F$	$\mathbf{A}_S\mathbf{B}_t\mathbf{D}_F$	$\mathbf{A}_S\mathbf{B}_{lt}\mathbf{D}_F$	$\mathbf{A}_S\mathbf{B}_S\mathbf{D}_F$	$\mathbf{A}_S\mathbf{B}_F\mathbf{D}_F$
$[+/-/-/+]_T$	$[+/\bigcirc/-_2/\bullet/+]_T$	$[+/-_3/+_2]_T$	$[+/\bigcirc_2/+/-_2/\bullet]_T$	$[+/-_2/+/\bigcirc]_T$	$[+/-/\bigcirc]_T$

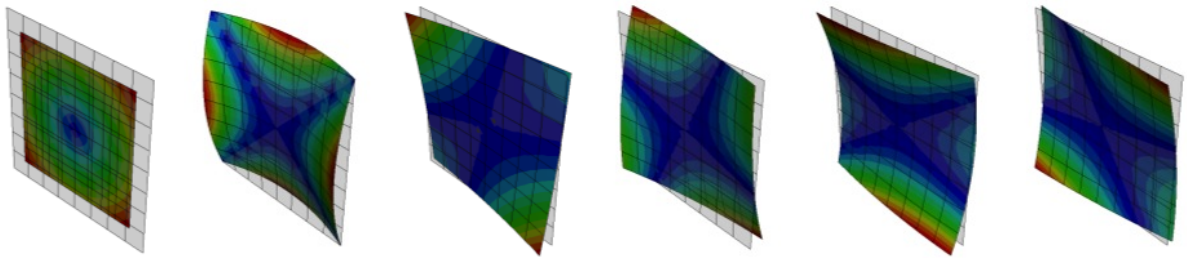

B-T laminate	*B-E;B-T*	*B-S-T-E;B-T*	*B-E-B-S-T-E;B-T*	*B-E-T-S;B-T*	*B-E-B-S-T-E-T-S;B-T*
$\mathbf{B} = \mathbf{0}$	$\begin{bmatrix} B_{11} & 0 & 0 \\ 0 & B_{22} & 0 \\ 0 & 0 & 0 \end{bmatrix}$	$\begin{bmatrix} 0 & 0 & B_{16} \\ 0 & 0 & B_{26} \\ B_{61} & B_{62} & 0 \end{bmatrix}$	$\begin{bmatrix} B_{11} & 0 & B_{16} \\ 0 & B_{22} & B_{26} \\ B_{61} & B_{62} & 0 \end{bmatrix}$	$\begin{bmatrix} B_{11} & B_{12} & 0 \\ B_{21} & B_{22} & 0 \\ 0 & 0 & B_{66} \end{bmatrix}$	$\begin{bmatrix} B_{11} & B_{12} & B_{16} \\ B_{21} & B_{22} & B_{26} \\ B_{61} & B_{62} & B_{66} \end{bmatrix}$

Coupling responses, due to free thermal contraction, for laminates with shearing-extension coupling (or *E-S* laminate) combined with:

$\mathbf{A}_F\mathbf{B}_0\mathbf{D}_S$	$\mathbf{A}_F\mathbf{B}_l\mathbf{D}_S$	$\mathbf{A}_F\mathbf{B}_t\mathbf{D}_S$	$\mathbf{A}_F\mathbf{B}_{lt}\mathbf{D}_S$	$\mathbf{A}_F\mathbf{B}_S\mathbf{D}_S$	$\mathbf{A}_F\mathbf{B}_F\mathbf{D}_S$
$[\pm/\bigcirc/-/\bigcirc/-_3/\bigcirc/-_3/\bigcirc/+]_T$	$[\pm/\bigcirc/-/\bigcirc/-_3/\bigcirc/-_3/\bullet/+]_T$	$[\pm/\bigcirc/-_3/\bigcirc/-/\bigcirc/-_3/\pm/\bigcirc/+]_T$	$[\pm/\bigcirc/-_3/\bigcirc/-/\bigcirc/-_3/\pm/\bullet/+]_T$	$[\pm/\bigcirc/-_7/+/\bullet]_T$	$[+/-_6/\bigcirc/-_2/\bullet/+]_T$

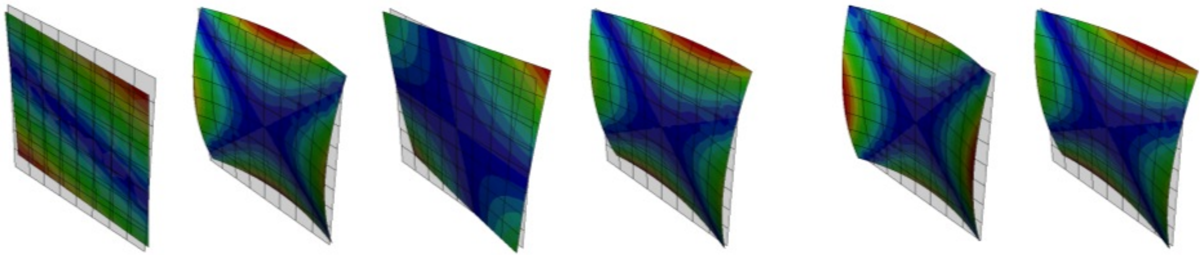

E-S laminate	*E-S*;*B-E*	*E-S*;*B-S*-*T-E*	*E-S*;*B-E*-*B-S*-*T-E*	*E-S*;*B-E*-*T-S*	*E-S*;*B-E*-*B-S*-*T-E*-*T-S*
$\mathbf{B} = \mathbf{0}$	$\begin{bmatrix} B_{11} & 0 & 0 \\ 0 & B_{22} & 0 \\ 0 & 0 & 0 \end{bmatrix}$	$\begin{bmatrix} 0 & 0 & B_{16} \\ 0 & 0 & B_{26} \\ B_{61} & B_{62} & 0 \end{bmatrix}$	$\begin{bmatrix} B_{11} & 0 & B_{16} \\ 0 & B_{22} & B_{26} \\ B_{61} & B_{62} & 0 \end{bmatrix}$	$\begin{bmatrix} B_{11} & B_{12} & 0 \\ B_{21} & B_{22} & 0 \\ 0 & 0 & B_{66} \end{bmatrix}$	$\begin{bmatrix} B_{11} & B_{12} & B_{16} \\ B_{21} & B_{22} & B_{26} \\ B_{61} & B_{62} & B_{66} \end{bmatrix}$

Coupling responses, due to free thermal contraction, for laminates with shearing-extension and bending-twisting coupling (or E-S;B-T laminate) combined with:

$\mathbf{A}_{\mathrm{F}}\mathbf{B}_0\mathbf{D}_{\mathrm{F}}$	$\mathbf{A}_{\mathrm{F}}\mathbf{B}_l\mathbf{D}_{\mathrm{F}}$	$\mathbf{A}_{\mathrm{F}}\mathbf{B}_t\mathbf{D}_{\mathrm{F}}$	$\mathbf{A}_{\mathrm{F}}\mathbf{B}_{lt}\mathbf{D}_{\mathrm{F}}$	$\mathbf{A}_{\mathrm{F}}\mathbf{B}_{\mathrm{S}}\mathbf{D}_{\mathrm{F}}$	$\mathbf{A}_{\mathrm{F}}\mathbf{B}_{\mathrm{F}}\mathbf{D}_{\mathrm{F}}$
[+/+]$_{\mathrm{T}}$	[+/○/●/+]$_{\mathrm{T}}$	[+/+/−]$_{\mathrm{T}}$	[+/○/+/●/−]$_{\mathrm{T}}$	[+/−/○/+/●]$_{\mathrm{T}}$	[+/○]$_{\mathrm{T}}$

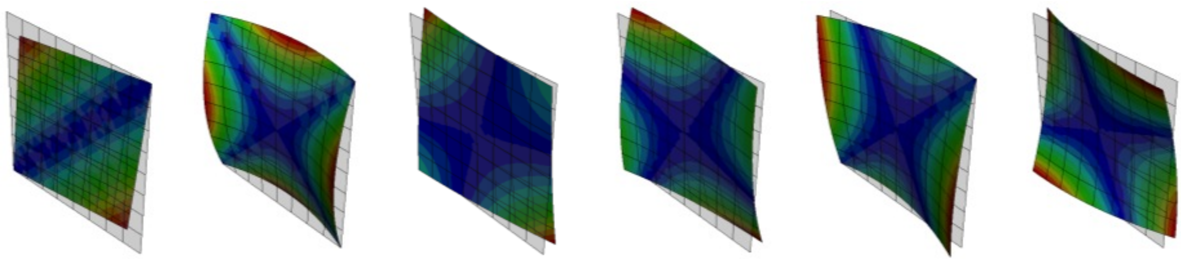

E-S;B-T laminate	E-S;B-E;B-T	E-S;B-S-T-E;B-T	E-S;B-E-B-S-T-E;B-T	E-S;B-E-T-S;B-T	E-S;B-E-B-S-T-E-T-S;B-T
$\mathbf{B} = \mathbf{0}$	$\begin{bmatrix} B_{11} & 0 & 0 \\ 0 & B_{22} & 0 \\ 0 & 0 & 0 \end{bmatrix}$	$\begin{bmatrix} 0 & 0 & B_{16} \\ 0 & 0 & B_{26} \\ B_{61} & B_{62} & 0 \end{bmatrix}$	$\begin{bmatrix} B_{11} & 0 & B_{16} \\ 0 & B_{22} & B_{26} \\ B_{61} & B_{62} & 0 \end{bmatrix}$	$\begin{bmatrix} B_{11} & B_{12} & 0 \\ B_{21} & B_{22} & 0 \\ 0 & 0 & B_{66} \end{bmatrix}$	$\begin{bmatrix} B_{11} & B_{12} & B_{16} \\ B_{21} & B_{22} & B_{26} \\ B_{61} & B_{62} & B_{66} \end{bmatrix}$

Experimental validation

Background on curvature predictions

Hyer[‡] discusses the suppression of the smaller of the two principal curvatures in experimental tests; for which Classical Lamination Theory (CLT) predicts a saddle shape.

Shown here is a *fully coupled* $\mathbf{A}_F\mathbf{B}_F\mathbf{D}_F$ laminate.

Note good agreement in the principal angle!

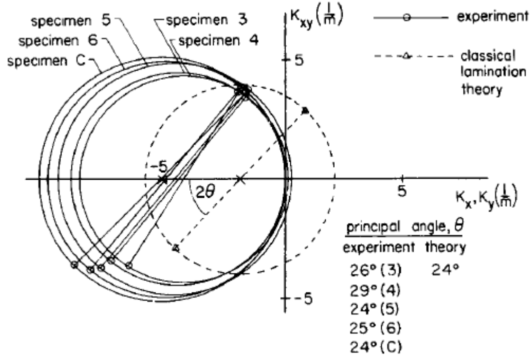

***Figure 5.** Curvature characteristics of $[0/90_2/45]_T$ laminates.*

‡ Hyer. M. W. (1981). Some observations on the cured shape of thin unsymmetric laminates, *Journal of Composite Materials*, **31**: 175-94

Stability

Hyer[§,**] explains the curvature suppression in terms of a critical side length – a geometric parameter, dependent on laminate thickness, which dictates the specific form of the room temperature shape.

A saddle shape is only physically stable for side lengths between points A and B on Fig. 5; this corresponds to the CLT prediction.
Thereafter, one of two stable cylindrical shapes exists, where the second is often achieved from the first by a simple snap-through action. Non-linear analysis is required to predict these shapes.

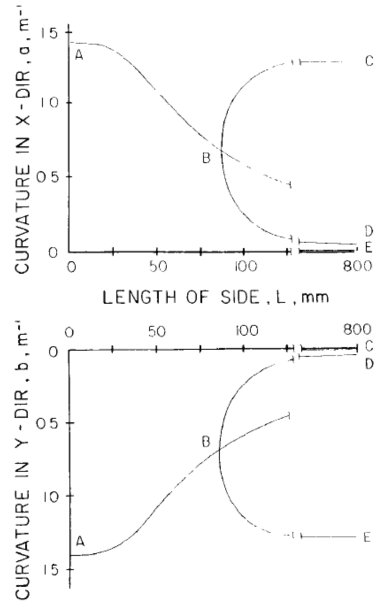

Figure 5. Room-temperature shapes of square [0/90/0/90]$_T$ laminates.

[§] Hyer, M. W. (1981). Calculations of the room-temperature shapes of unsymmetric laminates, *Journal of Composite Materials*, **15**: 296-310
[**] Hyer. M. W. (1982). The room-temperature shapes of four-layer unsymmetric cross-ply, *Journal of Composite Materials*, **16**: 318-40

New experimental observations on 380mm ✖ 380mm coupled specimens – Principal curvatures/directions derived from digitized surface profiles (3D laser scanner)

Sequence	κ_1 ($\times 10^{-6}$/mm)	κ_2 ($\times 10^{-6}$/mm)	θ_1 (°)	θ_2 (°)	Remarks
5. - $A_S B_l D_S$ $[+/-/\bigcirc/-/\bigcirc/+/\bullet/+/-]_T$	-455	19	-89	1	*Pseudo-Bistable*
6. - $A_S B_l D_F$ $[+/\bigcirc/-_2/\bullet/+]_T$	-3,400	-3	-25	65	*Pseudo-Bistable*
7. - $A_F B_l D_F$ $[+/\bigcirc/\bullet/+]_T$	-3,500	-5	-20	70	*Bistable*
	2,500	6	17	-73	
8. - $A_F B_l D_S$ $[\pm/\bigcirc/-/\bigcirc/-_3/\bigcirc/-_3/\bullet/+]_T$	466	-48	90	0	---

Pseudo-Bistable implies that a snap-though may be invoked, producing an audible 'click', but that a force must be continuously applied to prevent snap-back.

Sequence	κ_1 ($\times 10^{-6}$/mm)	κ_2 ($\times 10^{-6}$/mm)	θ_1 (°)	θ_2 (°)	Remarks
10. - $A_S B_t D_F$ $[+/-_3/+_2]_T$	-1,500	1	-42	48	---

Sequence	κ_1 ($\times 10^{-6}$/mm)	κ_2 ($\times 10^{-6}$/mm)	θ_1 (°)	θ_2 (°)	Remarks
16. - $A_F B_{lt} D_S$ $[\pm/\bigcirc/-_3/\bigcirc/-/\bigcirc/-_3/\pm/\bullet/+]_T$	473	-45	79	-11	---

Sequence	κ_1 ($\times 10^{-6}$/mm)	κ_2 ($\times 10^{-6}$/mm)	θ_1 (°)	θ_2 (°)	Remarks
18. - $A_S B_S D_F$ [+/−$_2$/+/○]$_T$	-2,900	-9	-73	17	*Pseudo-Bistable*
19. - $A_F B_S D_F$ [+/−/○/+/●]$_T$	-2,500	-2	-17	73	*Pseudo-Bistable*
20. - $A_F B_S D_S$ [±/○/−$_7$/+/●]$_T$	232	-170	-88	2	---

Sequence	κ_1 ($\times 10^{-6}$/mm)	κ_2 ($\times 10^{-6}$/mm)	θ_1 (°)	θ_2 (°)	Remarks
21. - $A_S B_F D_S$ [+/−$_2$/+/○/+/−/●]$_T$	-435	22	4	-86	*Pseudo-Bistable*

Test specimens:

5.

6.

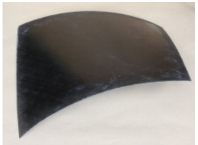

7.

8.

10.

16.

18.

19.

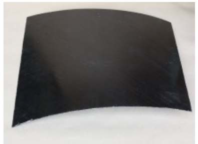

20.

21.

Laminate design

Hygro-thermally Curvature-Stable or Warp-Free Laminates

The manufacture of any of the foregoing coupled classes of laminate presents a particular challenge if mechanical coupling attributes are required without the thermal distortions illustrated; such distortions are a consequence of the high temperature curing process requirements.

Hygro-thermally curvature-stable (HTCS) or thermally warp-free laminates offer a tailored design solution. Note that uniform temperature and moisture change are synonymous in the context of the requirements for HTCS laminates.

To achieve the HTCS condition, we require square symmetry in **A**, **B** and **N**, with **M** = **0**.

Square symmetry implies equal stiffness on principal axes, as would be the case in a balanced cross-ply laminate or a fabric with balanced weave.

Square symmetry in the thermal load vector, **N**, implies thermally isotropic behaviour.

Square Symmetric forms for A and B matrices: Conditions for hygro-thermally curvature-stable behaviour in coupled laminates. Lamination parameters are given for comparison.

$\beta = m\pi/2$	$\beta = \pi/8 + m\pi/2$	$\beta \neq m\pi/2, \pi/8 + m\pi/2$
	$(m = 0, 1, 2, 3)$	
(A_S) $\begin{bmatrix} A_{11} & A_{12} & 0 \\ A_{21} & A_{11} & 0 \\ 0 & 0 & A_{66} \end{bmatrix}$ $\xi_1 = \xi_3 = \xi_4 = 0$		(A_F) $\begin{bmatrix} A_{11} & A_{12} & A_{16} \\ A_{21} & A_{11} & -A_{16} \\ A_{16} & -A_{16} & A_{66} \end{bmatrix}$ $\xi_1 = \xi_3 = 0$
(B_S) $\begin{bmatrix} B_{11} & -B_{11} & 0 \\ -B_{11} & B_{11} & 0 \\ 0 & 0 & -B_{11} \end{bmatrix}$ $\xi_5 = \xi_7 = \xi_8 = 0$	(B_t) $\begin{bmatrix} 0 & 0 & B_{16} \\ 0 & 0 & -B_{16} \\ B_{16} & -B_{16} & 0 \end{bmatrix}$ $\xi_5 = \xi_6 = \xi_7 = 0$	(B_F) $\begin{bmatrix} B_{11} & -B_{11} & B_{16} \\ -B_{11} & B_{11} & -B_{16} \\ B_{16} & -B_{16} & -B_{11} \end{bmatrix}$ $\xi_5 = \xi_7 = 0$

E-B-S-T coupled quasi-homogenous orthotropic laminates ($\mathbf{A}_S\mathbf{B}_S\mathbf{D}_S \rightarrow \mathbf{A}_I\mathbf{B}_S\mathbf{D}_I$)[††]

Quasi-homogenous orthotropic laminates → $D_{ij} = A_{ij}H^2/12$,

Hygro-thermally curvature-stable 16-ply quasi-homogeneous orthotropic stacking sequence configurations, together with the corresponding lamination parameter, ξ_6, representing $\mathbf{A}_I\mathbf{B}_S\mathbf{D}_I$ laminates with standard ply orientations ±45, 0 and 90° in place of symbols +, −, ○ and ●, respectively.

Stacking sequence	ξ_6
[+/−/−/+/−/+/+/−/○/●/●/○/●/○/○/●]$_T$ ≡ [+/−/−/+/−/+/+/−/●/○/○/●/○/●/●/○]$_T$	1.00
[+/−/−/+/○/●/●/○/−/+/+/−/●/○/○/●]$_T$ ≡ [+/−/−/+/●/○/○/●/−/+/+/−/○/●/●/○]$_T$	0.50
[+/−/○/●/−/+/●/○/−/+/●/○/+/−/○/●]$_T$ ≡ [+/−/●/○/−/+/○/●/−/+/○/●/+/−/●/○]$_T$	0.25
[+/○/−/●/−/●/+/○/−/●/+/○/+/○/−/●]$_T$ ≡ [+/●/−/○/−/○/+/●/−/○/+/●/+/●/−/○]$_T$	0.13

[††] York C. B. (2010). Coupled Quasi-Homogeneous Orthotropic Laminates. *Proc. 16th International Conference on Mechanics of Composite Materials,* Riga, Latvia.

E-B-S-T coupled extensionally isotropic laminates ($\mathbf{A}_I\mathbf{B}_S\mathbf{D}_S$)
$D_{ij} \neq A_{ij}H^2/12 \rightarrow$ 8, 264 and 17,118 sequences for n = 12, 16 and 20.

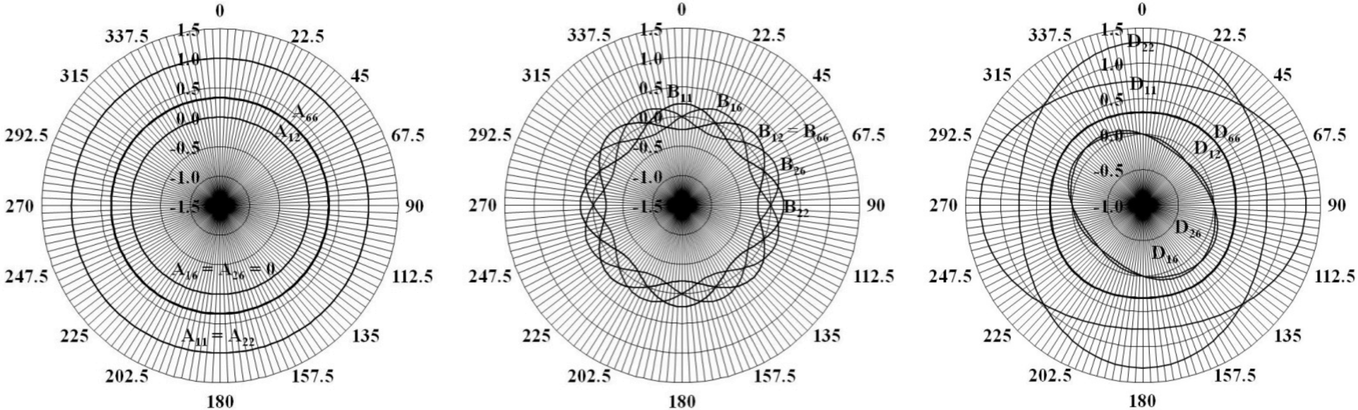

(a) A_{ij}/A_{Iso} (b) B_{ij}/B_{Iso} (c) D_{ij}/D_{Iso}

Polar plots of the stiffnesses for off-axis material alignment of $[-/+_2/\bigcirc/-_2/+/\bullet_3/\bigcirc_2]_T$.

E-B-S-T;B-T coupled extensionally isotropic laminates ($\mathbf{A}_I\mathbf{B}_S\mathbf{D}_F$)

D_{16}, $D_{26} \neq 0$ $\rightarrow$ 6, 280, 23,652 and 2,379,722 sequences with n = 8, 12, 16 and 20 plies.

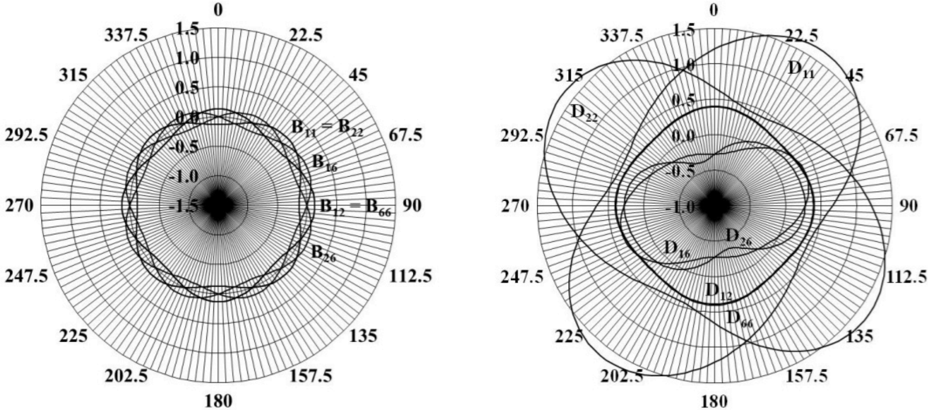

(a) B_{ij}/B_{Iso} (b) D_{ij}/D_{Iso}

Polar plots of the stiffnesses for off-axis material alignment of $[-/\bullet_2/\circ_3/+_3/\bullet/-_2]_T$.

<u>E</u>-<u>B</u>-<u>S</u>-<u>T</u> coupled laminates ($\mathbf{A}_S\mathbf{B}_S\mathbf{D}_S$)

A_{16}, $A_{26} \neq 0 \rightarrow$ 6, 524, and 35,610 solutions for n = 12, 16 and 20 ply laminates.

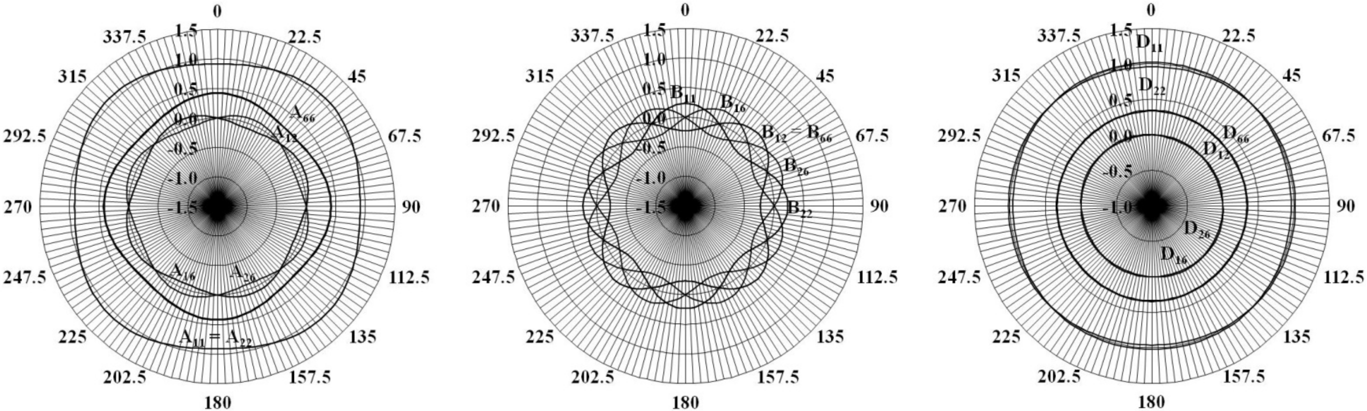

(a) A_{ij}/A_{Iso} (b) B_{ij}/B_{Iso} (c) D_{ij}/D_{Iso}

Polar plots of the stiffnesses for off-axis material alignment of [−/+/+/−/+/−/−/+/●/○/○/●]$_T$.
Note bending-twisting coupling closely approximates isotropic behaviour.

The [−/+/+/−/+/−/−/+/●/○/○/●]$_T$ stacking sequence is of particular interest in the context of aero-elastic compliant wind-turbine blade design, for passive load alleviation, where laminate level extension-shearing, extension-twisting (and shearing-bending) coupling provides the necessary and sufficient response to achieve bending-twisting and extension-twisting at the structural level, from aerodynamic and centripetal forces, respectively.

E-B-S-T;B-T coupled laminates ($\mathbf{A}_S\mathbf{B}_S\mathbf{D}_F$)

A_{16}, $A_{26} \neq 0$ and D_{16}, $D_{26} \neq 0$ gives 410, 40,808 and 4,515,473 solutions with n = 12, 16 and 20 plies.

New experimental observations on 380mm ✖ 380mm HTCS specimens – Principal curvatures/directions derived from digitized surface profiles (3D laser scanner)

Sequence	κ_1 ($\times 10^{-6}$/mm)	κ_2 ($\times 10^{-6}$/mm)	θ_1 (°)	θ_2 (°)	Remark
25. - $A_I B_S D_S$ [−/+$_2$/○/−$_2$/+/●$_3$/○$_2$]$_T$	51	-2	-74	16	---
27. - $A_S B_I D_S$ [−/+/+/−/+/−/−/+/●/○/○/●]$_T$	31	13	-48	42	---

Curvatures of this magnitude would arise due to a single (outer-) ply orientation error of 2°

Specimens tested:

25.

27.

Conclusions

Stacking sequence configurations for hygro-thermally curvature-stable laminates have been identified in **9** of the **24** classes of coupled laminate with standard ply angle orientations +45, −45, 0 and 90°. Additionally, **4** classes have **B** = **0**.

All 9 HTCS classes arise from the judicious re-alignment of the principal material axis of either $\mathbf{A}_S\mathbf{B}_S\mathbf{D}_S$ (or *B-E-T-S*) laminates, or $\mathbf{A}_S\mathbf{B}_S\mathbf{D}_F$ (or *B-E-T-S;B-T*) laminates.
Off-axis material alignment of these parent laminates gives rise to more complex combinations of mechanical coupling behaviour.

For standard ply angle orientations +45, −45, 0 and 90°, HTCS solutions were found in only 8-, 12-, 16- and 20-ply laminates. However, ply number groupings can be expanded by considering non-standard ply angle orientations +60, −60, 0 and 90°, leading to solutions in all ply number groupings with (*n* =) 10 plies and above.

A preliminary set of experimental results have been presented, that reveal:

- cylindrical room-temperature shapes are present in a broader range of coupled laminate classes than previously dicovered, and that at least one class appears to develop into a saddle shape at a relatively high side-length-to-thickness ratio;

- Bistable and Pseudo-Bistable Snap-through behaviour in a large proportion of the 24 classes of coupled laminate;
- HTCS laminates with a range of mechanical coupling attributes can be readily manufactured by hand lay-up and a standard high temperature curing process and will remain (*practically*) warp free.

Acknowledgements

Airbus (Composites Centre, Stade) is gratefully acknowledged for manufacturing the 30 proof of concept specimens which made this study possible.

Some additional specimen photographs exhibiting large/extreme curvatures:

9. – $\mathbf{A}_{\mathrm{S}}\mathbf{B}_{t}\mathbf{D}_{\mathrm{S}}$

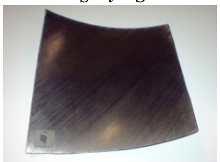

11. – $\mathbf{A}_{\mathrm{F}}\mathbf{B}_{t}\mathbf{D}_{\mathrm{F}}$

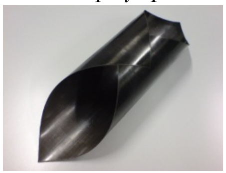

13. – $\mathbf{A}_{\mathrm{S}}\mathbf{B}_{lt}\mathbf{D}_{\mathrm{S}}$

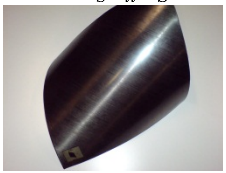

14. – $\mathbf{A}_{\mathrm{S}}\mathbf{B}_{lt}\mathbf{D}_{\mathrm{F}}$

24. – $\mathbf{A}_{\mathrm{F}}\mathbf{B}_{\mathrm{F}}\mathbf{D}_{\mathrm{S}}$

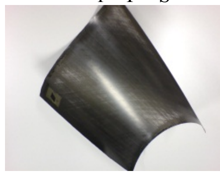

Appendix: Normalization of polar plots

Equivalent **FIL** properties are readily obtained from the laminate invariants expressed in terms of their isotropic material counterparts, where $E_1 = E_2$, $\nu_{12} = \nu_{21}$, etc:

$$E_{Iso} = 2(1 + \nu_{Iso})G_{Iso} = U_1(1 - \nu_{Iso}^2) \tag{1}$$

where

$$\nu_{Iso} = U_4/U_1 \tag{2}$$

and

$$G_{Iso} = U_5 \tag{3}$$

The Young's modulus, E_{Iso}, Poisson ratio, ν_{Iso}, and shear modulus, G_{Iso}, are the equivalent isotropic material properties of a composite laminate of thickness, H, corresponding to the total number of plies, n, of uniform thickness, t, and from which the equivalent isotropic stiffness properties for laminates with any number of plies then follows:

$$A_{Iso} = A_{11} = A_{22} = E_{Iso}H/(1 - \nu_{Iso}^2) = U_1 H \tag{4}$$

$$A_{12} = \nu_{Iso}A_{11} \tag{5}$$

$$A_{66} = U_5 H \tag{6}$$

and the bending stiffness elements follow from:

$$D_{Iso} = E_{Iso}H^3/12(1 - \nu_{Iso}^2) = U_1H^3/12 \qquad (7)$$

Equivalent **FIL** stiffness properties can be used to normalize the properties of other laminates. However for coupled laminates an expression for the equivalent B_{Iso} must be introduced:

$$B_{Iso} = E_{Iso}H^2/4(1 - \nu_{Iso}^2) = U_1H^2/4 \qquad (8)$$